Edward C. Emery,[1] Eleftheria Diakogiannaki,[1] Clive Gentry,[2] Arianna Psichas,[1] Abdella M. Habib,[3] Stuart Bevan,[2] Michael J.M. Fischer,[4] Frank Reimann,[1] and Fiona M. Gribble[1]

Stimulation of GLP-1 Secretion Downstream of the Ligand-Gated Ion Channel TRPA1

Diabetes 2015;64:1202–1210 | DOI: 10.2337/db14-0737

SIGNAL TRANSDUCTION

Stimulus-coupled incretin secretion from enteroendocrine cells plays a fundamental role in glucose homeostasis and could be targeted for the treatment of type 2 diabetes. Here, we investigated the expression and function of transient receptor potential (TRP) ion channels in enteroendocrine L cells producing GLP-1. By microarray and quantitative PCR analysis, we identified *trpa1* as an L cell–enriched transcript in the small intestine. Calcium imaging of primary L cells and the model cell line GLUTag revealed responses triggered by the TRPA1 agonists allyl-isothiocyanate (mustard oil), carvacrol, and polyunsaturated fatty acids, which were blocked by TRPA1 antagonists. Electrophysiology in GLUTag cells showed that carvacrol induced a current with characteristics typical of TRPA1 and triggered the firing of action potentials. TRPA1 activation caused an increase in GLP-1 secretion from primary murine intestinal cultures and GLUTag cells, an effect that was abolished in cultures from *trpa1*$^{-/-}$ mice or by pharmacological TRPA1 inhibition. These findings present TRPA1 as a novel sensory mechanism in enteroendocrine L cells, coupled to the facilitation of GLP-1 release, which may be exploitable as a target for treating diabetes.

The global rise in the prevalence of type 2 diabetes makes it one of the biggest health and socioeconomic burdens of the 21st century. One of the newest and most successful strategies for the treatment of type 2 diabetes is based on mimicking, or enhancing, the endogenous action of incretin hormones. Glucose-dependent insulinotropic peptide (GIP) and GLP-1 are incretin peptides released from K and L cells, respectively, located in the epithelial layer of the gastrointestinal tract. GIP and GLP-1 potentiate glucose-dependent insulin secretion, whereas GLP-1 additionally suppresses appetite, glucagon secretion, and gastric emptying (1). These effects have been exploited pharmacologically through the use of long-acting GLP-1 mimetics or inhibitors of incretin inactivation by dipeptidyl peptidase-4 (DPP4) (2). Incretin therapy has significant benefits over older insulinotropic medications like sulphonylureas, as it does not bypass the glucose-sensing machinery of the pancreatic β-cell and thus promotes insulin secretion in relation to ambient plasma glucose levels, minimizing the risk of hypoglycemia. In addition, GLP-1 mimetics are associated with sustained weight loss (3,4), whereas DPP4 inhibitors appear to be weight neutral (5), a difference that might reflect the higher effective concentrations of active GLP-1 reached with the former. Importantly, the substantially increased release of endogenous GLP-1 seen after Roux-en-Y gastric bypass surgery is likely to contribute toward the observed high rates of resolution of type 2 diabetes (6,7). Understanding the mechanisms that underlie endogenous GLP-1 secretion could therefore facilitate the development of novel therapies based on potentiating the postprandial incretin effect.

Over the past decade, we and others have investigated the mechanisms underlying nutrient-coupled incretin secretion (8), aided by the development of model enteroendocrine cells lines (including GLUTag and STC-1) as well as primary intestinal epithelial cell cultures. As hormone

[1]Cambridge Institute for Medical Research, Addenbrooke's Hospital, Cambridge, U.K.
[2]Wolfson Centre for Age-Related Diseases, King's College London, London, U.K.
[3]Molecular Nociception Group, Wolfson Institute for Biomedical Research, University College London, London, U.K.
[4]Institute of Physiology and Pathophysiology, University of Erlangen-Nuremberg, Erlangen, Germany

Corresponding authors: Fiona M. Gribble, fmg23@cam.ac.uk, and Frank Reimann, fr222@cam.ac.uk.

Received 8 May 2014 and accepted 8 October 2014.

This article contains Supplementary Data online at http://diabetes.diabetesjournals.org/lookup/suppl/doi:10.2337/db14-0737/-/DC1.

release is dependent upon elevated cytosolic Ca^{2+}, mechanisms of stimulus-coupled incretin secretion are commonly associated with membrane depolarization and voltage-gated Ca^{2+} channel activation, or the release of Ca^{2+} from intracellular stores (9–12). Although numerous ion channels and G protein–coupled receptors (GPCRs) have been shown to facilitate these mechanisms, the potential contribution of the transient receptor potential (TRP) superfamily of ion channels has been relatively unexplored. TRP ion channels form a family of nonselective, cation-conducting channels that are responsive to a variety of physical, chemical, and thermal stimuli and play fundamental roles in sensory physiology (13). They have well-established roles in conferring appreciation for bitter, sweet, and umami tastes (14), as well as the regulation of gastrointestinal motility and absorption (15). Emerging data support a role for TRP channels in modulating both incretin and insulin secretion. Oral administration of the TRPV1 agonist capsaicin, for example, increased plasma GLP-1 and insulin concentrations and improved glucose tolerance in mice (16). TRPA1 agonists have been shown to regulate insulin secretion from rat pancreatic β-cells and to increase peptide YY (PYY) release and suppress food intake and gastric emptying in mice (17,18). TRPA1 is well characterized as a detector of nonnutrient food components such as cinnamaldehyde (cinnamon), gingerol (ginger), allicin (garlic), and allyl-isothiocyanate (AITC, mustard oil) but has also been identified as a putative polyunsaturated fatty acid (PUFA) sensor (19,20). Doses (1 and 3 g) of cinnamon were found to increase GLP-1 levels in humans (21). Despite these findings, however, the functional contribution of TRP channels to the regulation of enteroendocrine cell physiology is currently unclear.

In this study, we investigated the expression and function of TRP channels in enteroendocrine cells. We show that *trpa1* is selectively expressed in L cells of the small intestine, is functionally active, and is involved in nutrient- and nonnutrient-coupled GLP-1 secretion.

RESEARCH DESIGN AND METHODS

Animals

Animal procedures were approved by local ethical review committees and conformed to U.K. Home Office regulations. Experiments were performed using mice on a C57B/6 background. *Trpa1*$^{-/-}$ mice were a gift from Drs. Kelvin Kwan and David Corey (Harvard Medical School, Boston, MA) (22). GLU-Cre mice have been described previously (23). To enable Ca^{2+} monitoring in small intestinal L cells, these were crossed with commercially available ROSA26-GCaMP3 reporter mice (24) (Jax stock 014538), resulting in expression of the genetically encoded Ca^{2+} sensor in L cells, and with ROSA26-tdRFP mice to facilitate L-cell identification (25).

Primary Enteroendocrine and GLUTag Cell Culture

Processing and culture of primary enteroendocrine cells were as described previously (26). In brief, mice aged 10–24 weeks were killed by cervical dislocation, and colonic (entire colon/rectum), ileal (10-cm region adjacent to cecum), or duodenal (10-cm region adjacent to stomach) tissue was taken. Intestinal tissue was cleaned thoroughly with PBS and the outer muscle layer removed. Tissue was digested using collagenase type XI, and cell suspensions were plated either onto 24-well plates (GLP-1 secretion analysis) or 35-mm glass-bottomed dishes (Ca^{2+} imaging), pretreated with 1% volume for volume matrigel (BD Biosciences, Oxford, U.K.). For ileal and duodenal cultures, the ROCK inhibitor Y-27632 dihydrochloride (10 μmol/L) was added to final cell suspensions before plating.

GLUTag cells were maintained in 75-cm^2 flasks with DMEM (1,000 mg/L glucose) supplemented with 10% FBS, L-glutamine, and penicillin/streptomycin at 37°C, 5% CO_2. Cells for experimental use were plated as described for primary cultures or for electrophysiology were plated onto 35-mm plastic dishes. All cultures were analyzed within 48 h of plating.

Compounds

AITC, carvacrol, arachidonic acid (AA), eicosapentaenoic acid (EPA), docosahexaenoic acid (DHA), HC-030031, and A-967079 and other reagents, except where indicated, were obtained from Sigma-Aldrich (Poole, U.K.). For in vitro experiments, stock solutions (×1,000 working concentration) of AITC, AA, EPA, and DHA were made in DMSO, and carvacrol was made in ethanol. Compounds were diluted to working concentrations on the day of use. Respective vehicle controls were used to confirm the specificity of each compound tested.

Microarray Analysis

Isolated RNA from cell populations of different intestinal regions was extracted as previously described and converted to cDNA, which was then used for microarray analysis (27) using Affymetrix Murine 430 2.0 and Affymetrix ST 1.0 GeneChips.

Quantitative RT-PCR

Isolation and extraction of RNA were performed as previously described (27). The appropriate amount of first-strand cDNA template was mixed with specific TaqMan primers (Applied Biosystems, Foster City, CA), water, and PCR Master Mix (Applied Biosystems), and quantitative RT-PCR was conducted using a 7900HT Fast Real-Time PCR system (Applied Biosystems). Results were normalized to β-actin from the same sample. The following primer pairs were used (Applied Biosystems): *trpa1*, Mm01227437_m1; *trpc1*, Mm00441975_m1; *trpc3*, Mm00444690_m1; and *trpm7*, Mm00457998_m1. Experiments were performed on at least three independently isolated cDNA samples.

Ca^{2+} Imaging

GLUTag cells were incubated with 5 μmol/L fura-2-acetoxymethyl ester (fura-2-AM; Invitrogen, Paisley, U.K.) and 1 mmol/L glucose in standard extracellular buffer (concentrations in mmol/L: 143.4 NaCl, 4.5 KCl, 2.6 $CaCl_2$, 1.2 $MgCl_2$, and 10 HEPES, pH corrected to 7.4 using NaOH) for 15 min at 37°C followed by 15 min at

room temperature. Cells were then washed three times with glucose-free extracellular solution (as above), and changes in Ca^{2+} levels were assessed by measuring the change in ratiometric fluorescence (excitation 340 ± 10/380 ± 4 nm) at ≥510 nm. Measurements of intracellular Ca^{2+} dynamics from primary cultures were performed using intestinal cultures from GLU-Cre/ROSA26-GCaMP3/ROSA26-tdRFP mice. L cells were identified by the presence of RFP fluorescence, and changes in intracellular Ca^{2+} levels were represented by a change in the intensity of GFP fluorescence (excitation 480 ± 10 nm). Imaging experiments were performed using an Olympus IX71 microscope with a 40× oil immersion objective, fitted with a monochromator (Cairn Research, Faversham, U.K.) and OrcaER camera (Hamamatsu, Hamamatsu City, Japan). Images were acquired at 1 Hz and analyzed, after background subtraction, using MetaFluor software (Molecular Devices, Sunnyvale, CA).

Electrophysiological Analysis

Electrophysiological experiments were performed using an Axopatch 200B and Digidata 1440A (Axon Instruments, Sunnyvale, CA). Fire-polished filamented borosilicate patch pipettes coated with beeswax, with a resistance of 2.5–4 mol/LΩ, were used (Harvard Apparatus, Holliston, MA). For current clamp experiments, the following solutions were used: standard extracellular buffer, as above, and intracellular solution (in mmol/L): 107 KCl, 1 $CaCl_2$, 7 $MgCl_2$, 11 EGTA, 10 HEPES, and 5 K_2ATP (pH 7.2 with KOH). For voltage clamp experiments, following whole-cell configuration, series resistance was compensated by 70% and the following solutions were used: extracellular solution (in mmol/L), 115 NaCl, 5 CsCl, 5 $CoCl_2$, 20 TEA-Cl_2, 10 4-aminopyridine, 5 EDTA, 10 HEPES, and 0.3 μmol/L tetrodotoxin (pH 7.4 with NaOH); and intracellular solution (in mmol/L), 107 CsCl, 5 $MgCl_2$, 11 EGTA, 10 HEPES, and 5 Na_2ATP (pH 7.2 with CsOH). Recordings were acquired at 25 kHz and filtered (low-pass Bessel filter) at 10 kHz.

GLP-1 Analysis From Primary Intestinal and GLUTag Cultures

After 24 h in culture, wells were washed three times with standard extracellular buffer supplemented with 0.1% BSA (fatty acid free) and 10 mmol/L glucose. Test compounds were diluted to their working concentration in the same extracellular buffer and added to each well (250 μL). Cells were incubated at 37°C for 2 h, and solutions were then removed and centrifuged at 2,000 RCF for 5 min. Supernatants were snap frozen on dry ice. For primary intestinal cultures, supernatant and lysate samples were collected. GLP-1 contents were measured using a total GLP-1 assay (Meso Scale Discovery, Gaithersburg, MD). For primary cultures, results were calculated as a percentage of GLP-1 content per well and were normalized to the control well (extracellular buffer alone) measured in parallel on the same day. For experiments where voltage-gated ion channels were blocked, the extracellular solution was replaced with that used for voltage clamp analysis (see above).

Assessment of GLP-1 Release In Vivo

Male mice were fasted overnight before receiving AITC or vehicle (PBS) by oral gavage (10 mL/kg). Five minutes after the gavage, each animal was anesthetized (isoflurane) and a terminal blood sample was taken. For intestinal perfusion studies, fasted male mice were anesthetized and underwent a laparotomy prior to receiving an intraduodenal bolus injection (0.6 mL) of carvacrol, vehicle (PBS), or positive control (20% weight for volume glucose in PBS). A portal vein blood sample was taken at 5 min postinjection. The method was adapted from a protocol previously described for colonic stimulation (28). Blood samples were collected in EDTA and centrifuged at 13,000*g* for 90 s, and the plasma was collected and used for GLP-1 analysis.

Data Analysis

Results are expressed as mean ± SEM, unless otherwise stated. Statistical analysis was performed using GraphPad Prism (version 5.01, San Diego, CA). For mRNA expression and GLP-1 secretion data, one-way ANOVA with Bonferroni post hoc analysis was performed on log-transformed values, as these data were heteroscedastic. Electrophysiological and Ca^{2+} imaging data were assessed using repeated-measures ANOVA with Bonferroni post hoc analysis or paired Student *t* test, as appropriate. Values were regarded as significant if $P < 0.05$.

RESULTS

TRP Expression Profiles Within Discrete Enteroendocrine Cell Populations

Microarray analysis was used to compare expression of mRNAs encoding TRP channels in primary murine K- and L-cell populations as well as in GLUTag and STC-1 cell lines (27). The profiling of TRP channel expression using the Affymetrix 430 2.0 array is shown in Fig. 1. Of the 24 channels analyzed, only 6 (*trpa1*, *trpc1*, *trpc3*, *trpc4*, *trpc5*, and *trpm7*) exhibited at least twofold higher expression in one or more primary enteroendocrine cell populations compared with their respective negative controls. An independent microarray analysis of L cells and controls from the upper small intestine was performed using Affymetrix ST 1.0 arrays (Supplementary Fig. 1*A*) and confirmed the selective and/or high expression of *trpa1*, *trpc1*, *trpc3*, and *trpm7*, but not *trpc4* and *trpc5*. Of the four candidates identified from both screens, TRPA1 is the only channel currently known to be potently activated by compounds commonly present in food and was therefore chosen for further investigation. In contrast to a previous report (16), which detected TRPV1 immunohistochemically in STC-1 cells, we only found very low *trpv1* mRNA expression in all the analyzed cell types, with no evidence of enteroendocrine cell–specific expression.

To confirm the fidelity of the microarray screens, targeted quantitative PCR was performed to assess *trpa1* expression levels in L cells of the small and large intestine as well as in GLUTag cells (Fig. 1, inset). As observed in the microarray screen, *trpa1* expression was enriched in L-cell populations compared with controls, was higher

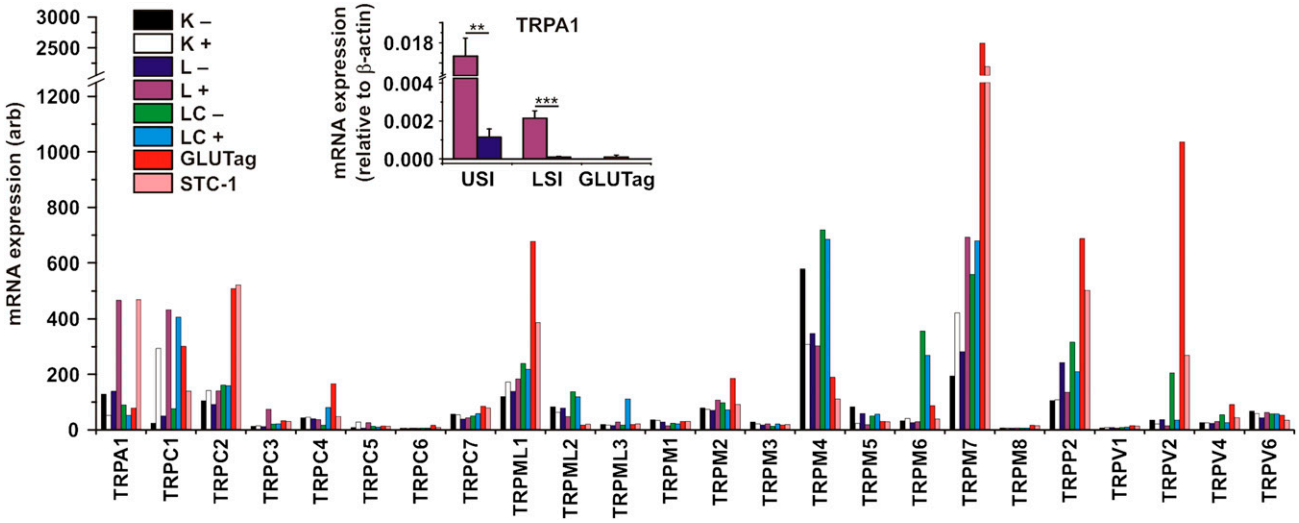

Figure 1—Expression profiles of TRP channel mRNAs within discrete enteroendocrine cell populations. Main figure shows microarray analysis for the TRP superfamily. Expression of each TRP mRNA was assessed by robust multiarray analysis from murine small intestinal K (K+) and L (L+) cells, colonic L cells (LC+), as well as GLUTag and STC-1 cell lines. Each primary enteroendocrine cell population was compared with their respective negative population (K−, L−, and LC−). Inset shows real-time quantitative PCR analysis of *trpa1* mRNA in the upper small intestine (USI) and lower small intestine (LSI) within murine L+ and L− cell populations, as well as GLUTag cells. Values are normalized to the expression of β-actin from the same cell populations ($n \geq 3$; $^{**}P < 0.01$ and $^{***}P < 0.001$, two-way unpaired Student *t* test). arb, arbitrary units.

in upper than in lower small intestinal L cells, and was detectable at low levels in GLUTag cells. It was not detectable in colonic L cells (data not shown). Expression of *trpc1*, *trpc3*, and *trpm7* was also confirmed using targeted quantitative analysis, further validating the expression profiles identified by the microarrays (Supplementary Fig. 1*B–D*).

Ca^{2+} Response Following TRPA1 Agonism in Primary Enteroendocrine Cells

To assess whether the high expression of *trpa1* mRNA in upper small intestinal L cells represents a functional TRPA1 ion channel population, calcium imaging was performed on primary L cells cultured from the duodenum of GLU-Cre/ROSA26-GCaMP3 mice. These mice exhibit L cell–specific expression of the GCaMP3 protein, a genetically encoded Ca^{2+} sensor that enables intracellular Ca^{2+} levels to be monitored as a function of GFP fluorescence (24) (Fig. 2*A*). Consistent with the high expression of *trpa1* mRNA, the TRPA1 agonist AITC (100 μmol/L) caused a significant increase in GCaMP3 fluorescence in GLU-Cre/ROSA26-GCaMP3 primary L cells (Fig. 2*B* and Supplementary Fig. 2). This response was completely inhibited when AITC was coapplied with the specific TRPA1 inhibitor, A-967079 (10 μmol/L). To further validate the functional expression of TRPA1 ion channels, the action of an alternative agonist, carvacrol (50 μmol/L), was investigated. As observed following the application of AITC, carvacrol induced a large Ca^{2+} transient in GLU-Cre/ROSA26-GCaMP3 primary L cells, which was also completely inhibited following TRPA1 inhibition (Fig. 2*C*). To confirm the specificity of TRPA1 inhibition by A-967079, we tested its effects on responses to glucose. Consistent with previous findings (26), 10 mmol/L glucose caused an increase in intracellular Ca^{2+} in L cells, an effect that was reproducible and unaffected by the coapplication of A-967079 (Fig. 2*D*).

As TRPA1 has been reported to respond to a number of PUFAs (19), we examined the effects of AA, EPA, and DHA on duodenal GLU-Cre/ROSA26-GCaMP3 primary L cells. AA, EPA, and DHA (200 μmol/L each) caused robust increases in intracellular Ca^{2+} (Fig. 2*E–G*). Whereas the increase of intracellular Ca^{2+} caused by AA and EPA was prevented by A-967079, the effect of DHA was only partially inhibited, suggesting the additional activation of a TRPA1-independent mechanism.

We hypothesized that the Ca^{2+} responses could arise from direct Ca^{2+} entry through TRPA1, recruitment of intracellular Ca^{2+} stores, or depolarization-dependent activation of voltage-gated Ca^{2+} channels. When we used a cocktail of inhibitors (see RESEARCH DESIGN AND METHODS) to prevent activation of voltage-gated ion channels, AITC (100 μmol/L) failed to elicit a response (Fig. 2*H*), whereas bombesin (100 nmol/L), a Gq activator releasing Ca^{2+} from intracellular stores, still increased intracellular Ca^{2+} levels. These findings suggest that TRPA1 activation increases depolarization-dependent voltage-gated Ca^{2+} entry.

We investigated whether GLUTag cells could be used as a model system for monitoring TRPA1 activity. Despite the relatively low expression of *trpa1* mRNA, AITC induced robust calcium transients in a subpopulation (20/107; 19%) of GLUTag cells, supporting their use for the electrophysiological characterization of TRPA1.

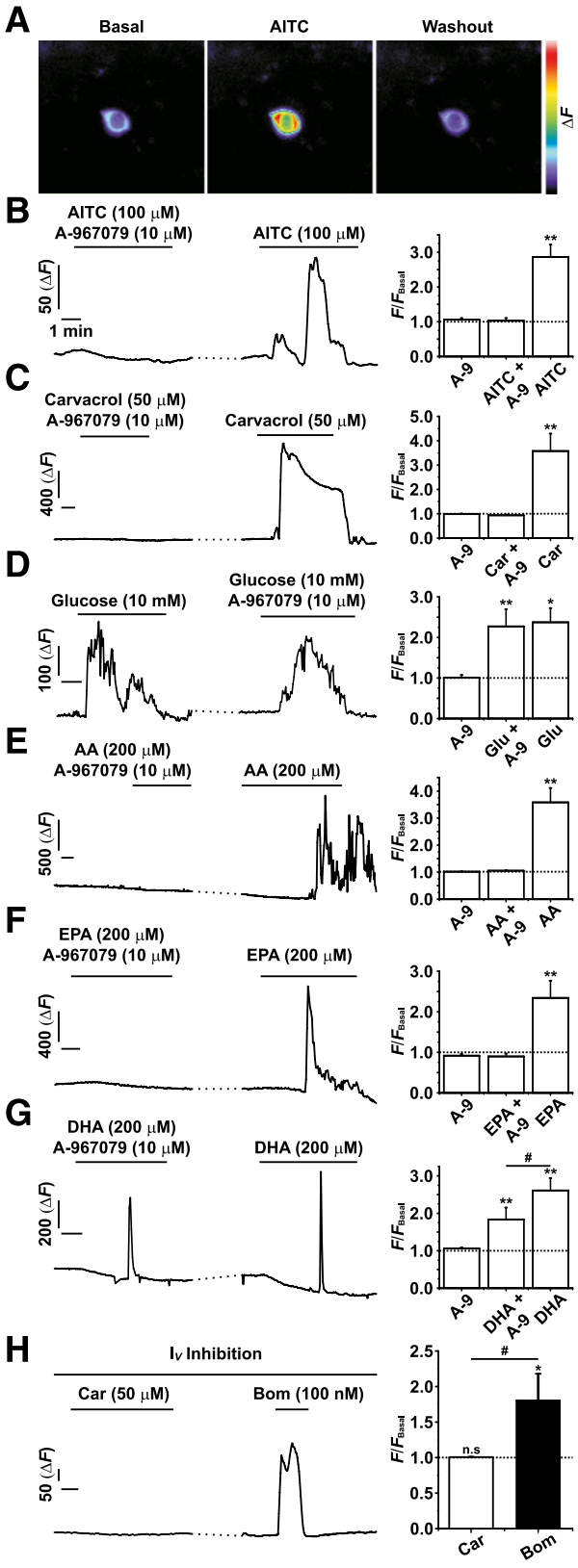

Figure 2—Ca^{2+} imaging analysis of TRPA1 in primary small intestinal L cells using GLU-Cre/ROSA26-GCaMP3 mice. *A*: Representative images showing the change in GCaMP3 fluorescence before, during, and after the application of AITC (100 μmol/L) to a primary duodenal L cell cultured from GLU-Cre/ROSA26-GCaMP3 mice. *B* and *C*: The application of AITC (100 μmol/L) or carvacrol (Car, 50 μmol/L) caused a robust and significant increase in intracellular Ca^{2+} as measured by GCaMP3 fluorescence, an effect that was inhibited by the coapplication of the TRPA1 inhibitor A-967079 (A-9, 10 μmol/L). *D*: Glucose (10 mmol/L) application significantly increased intracellular Ca^{2+} levels independent of TRPA1 inhibition. *E–G*: The addition of PUFAs AA, EPA, and DHA (all at 200 μmol/L) significantly increased intracellular Ca^{2+} levels. The coapplication of A-9 fully inhibited the effects of AA and EPA but only partially inhibited the effect of DHA on intracellular Ca^{2+} levels. *H*: Carvacrol (50 μmol/L) caused no change in intracellular Ca^{2+} levels during a complete voltage-gated ion channel block (see RESEARCH DESIGN AND METHODS). In contrast, the subsequent application of the Gq activator bombesin (Bom, 100 nmol/L) did cause a significant increase in intracellular Ca^{2+} levels. All experiments were $n \geq 5$. $^{*}P < 0.05$, #$P < 0.05$, and $^{**}P < 0.01$, repeated-measures ANOVA with Bonferroni post hoc test; *significance level from baseline; #significance level between groups. The dotted line on each graph represents the respective baseline value.

TRPA1 Agonists Potentiate Electrical Activity in GLUTag Cells

GLUTag cells were used to investigate whether TRPA1 activation modifies cellular electrical activity. Due to its ability to activate TRPA1 reversibly through noncovalent interactions (20), the effect of carvacrol (50 μmol/L) on action potential frequency was assessed using whole-cell current clamp. Carvacrol application caused a rapid increase in the rate of action potential firing from GLUTag cells, which was quickly reversed following washout (Fig. 3*A* and *B*). Subsequent responses to a glucose stimulus were unaffected (Fig. 3*A*). The carvacrol-triggered increase in action potential frequency was associated with depolarization of the resting membrane potential (from –54.9 ± 0.9 to –46.9 ± 1.3 mV, $n = 4$), consistent with the activation of a TRPA1-like depolarizing current (Fig. 3*B*) (29).

To further investigate the origin of the membrane depolarization, current-voltage analysis was performed on GLUTag cells using whole-cell voltage clamp. To isolate TRPA1-like currents, blockers of voltage-gated Na^+, K^+, and Ca^{2+} channels were used (see RESEARCH DESIGN AND METHODS). Addition of carvacrol activated an outwardly rectifying current, with characteristics typical of TRPA1 (Fig. 3*C* and *D*) (20), and was reversed by coapplication of A-967079 (10 μmol/L). Consistent with the observed shift in resting membrane potential and increase in action potential frequency, carvacrol significantly increased the magnitude of the depolarizing current measured at –50 mV, the typical resting membrane potential of GLUTag cells (30).

TRPA1 Agonist-Coupled GLP-1 Secretion in Enteroendocrine Cells

In GLUTag cells, AITC (100 μmol/L) caused an approximately twofold increase in GLP-1 secretion, independent of the basal glucose concentration (Fig. 4*A* and Supplementary Fig. 3*A*). This response was completely inhibited when AITC was coapplied with the TRPA1 inhibitor HC-030031 (50 μmol/L). Importantly, HC-030031 did not impair secretion triggered by glucose, consistent

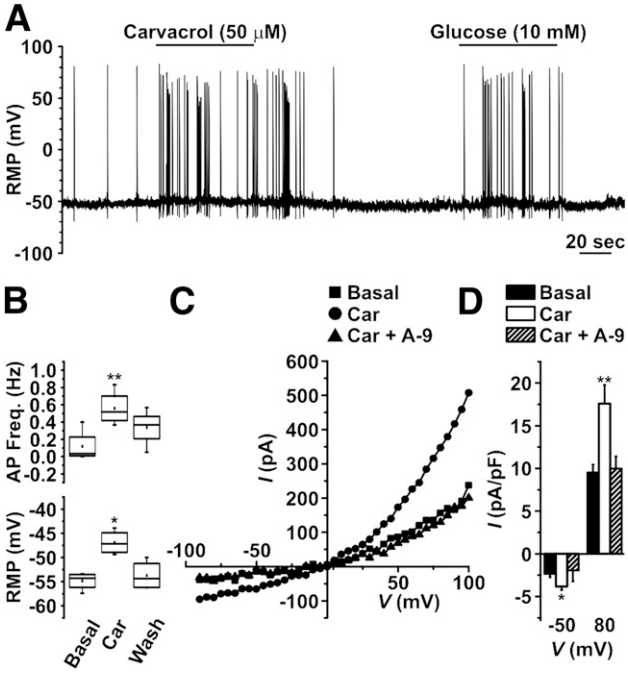

Figure 3—Electrophysiological analysis of TRPA1 in GLUTag cells. *A*: Representative current-clamp recording showing the increase in action potential frequency following the application of TRPA1 agonist carvacrol (50 μmol/L). The effect of carvacrol was reversible and did not affect responses to the subsequent application of glucose (10 mmol/L). *B*: The addition of carvacrol (Car) significantly and reversibly increased action potential frequency (AP Freq.) and depolarized the plasma membrane ($n = 4$). *C*: Representative current-voltage trace showing the effects of carvacrol application on increasing the outward- and inward-rectifying properties of an isolated TRP-like current. The change in rectification properties was fully reversed following the coapplication of A-967079 (A-9, 10 μmol/L). *D*: Carvacrol caused a significant increase in the inward current at −50 mV (typical resting membrane potential [RMP]) and outward current at +80 mV, which was reversed following the coapplication of A-967079 ($n = 7$; $^*P < 0.05$ and $^{**}P < 0.01$, two-way paired Student *t* test).

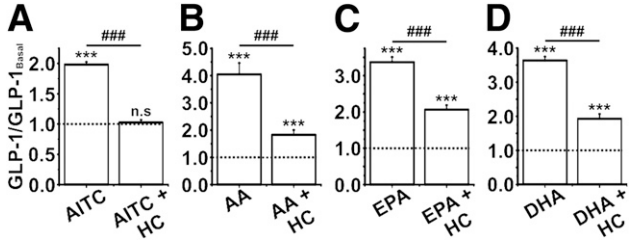

Figure 4—The effect of TRPA1 agonism on GLP-1 secretion from GLUTag cells. *A*: AITC (100 μmol/L) incubation with GLUTag cells caused a significant increase in GLP-1 secretion over 2 h, which was fully inhibited when AITC was coincubated with HC-030031 (HC, 50 μmol/L). *B–D*: The incubation of PUFAs AA, EPA, and DHA (all at 200 μmol/L) also caused a significant and robust increase in GLP-1 secretion from GLUTag cells. The coincubation with A-967079 significantly reduced, but did not abolish, the effect of PUFA-induced GLP-1 secretion. All experiments were $n \geq 6$. ***/###$P < 0.001$, one-way ANOVA with Bonferroni post hoc test; *significance level from baseline, #significance level between groups. The dotted line on each graph represents the respective baseline value. n.s., not significant.

with the lack of effect of TRPA1 antagonism on glucose-induced Ca^{2+} responses (Supplementary Fig. 3*B* and Fig. 2*D*). AA, EPA, and DHA (200 μmol/L each) all caused approximately fourfold elevations in GLP-1 secretion, which were significantly inhibited by coapplication of HC-030031 (Fig. 4*B–D*).

We next tested the response of primary ileal epithelial cultures to TRPA1 stimulation. Consistent with the effects observed in GLUTag cells, both AITC and carvacrol caused a significant increase in GLP-1 release, which was inhibited by HC-030031 (Fig. 5*A* and *B*). AITC failed to trigger GLP-1 secretion when Ca^{2+} entry through voltage-gated Ca^{2+} channels was prevented, whereas bombesin still enhanced GLP-1 secretion (Fig. 5*D*). Application of AA, EPA, and DHA also caused a significant increase in GLP-1 release, greater than that observed following AITC or carvacrol stimulation (Fig. 5*C*, *E*, and *F*). However, unlike in GLUTag cells, PUFA-stimulated GLP-1 secretion from ileal cultures was unaffected by HC-030031. To further confirm that the stimulatory effects of AITC and carvacrol were TRPA1 specific, ileal cultures were tested from *trpa1*$^{-/-}$ mice. Both AITC and carvacrol induced significantly smaller increases in GLP-1 release from *trpa1*$^{-/-}$ ileal cultures compared with age-matched *trpa1*$^{+/+}$ littermates, mirroring the reduced level of GLP-1 secretion observed following TRPA1 inhibition with HC-030031 (Fig. 5*G* and *H*). Application of 15 mg/kg AITC by gavage increased plasma GLP-1 concentrations in vivo, but this response was not reduced in *trpa1*$^{-/-}$ mice, whereas lower doses did not significantly increase GLP-1 levels (Fig. 6*A* and *B*). Injection of carvacrol directly into the duodenum of anesthetized mice, bypassing potential problems with gastric emptying, also only produced a trend toward increased GLP-1 secretion (Fig. 4*A* and *B*).

TRPV1 Agonism Has No Effect on Intracellular Ca^{2+} Levels or GLP-1 Secretion in Enteroendocrine L Cells

High concentrations of AITC have been shown to activate TRPV1 (31), and TRPV1 activation by capsaicin has been reported to increase plasma GLP-1 concentrations in mice (16). We therefore examined whether TRPV1 channels are functionally expressed in L cells and might account for the observed nonspecific increase in plasma GLP-1 levels by AITC in vivo. Consistent with the low *trpv1* mRNA levels, however, application of the specific TRPV1 agonist capsaicin (100 nmol/L) caused no change in GCaMP3 fluorescence in primary colonic L cells (Fig. 7*A*). Furthermore, incubation of primary ileal, colonic, or GLUTag cultures with capsaicin (100 nmol/L) did not increase GLP-1 secretion (Fig. 7*B*).

DISCUSSION

Trpa1 was identified by expression analysis as an enteroendocrine cell transcript localized particularly to L cells of the upper small intestine. In functional experiments, TRPA1 activation was shown to cause membrane depolarization, action potential firing, Ca^{2+} entry, and GLP-1 secretion. Responses were triggered by AITC and carvacrol

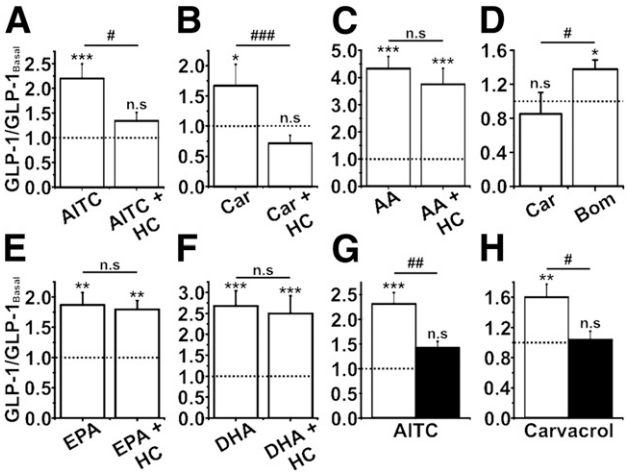

Figure 5—The effect of TRPA1 agonism on GLP-1 secretion from small intestinal *trpa1*$^{+/+}$ and *trpa1*$^{-/-}$ enteroendocrine cells. *A* and *B*: Both AITC (100 μmol/L) and carvacrol (50 μmol/L) caused a significant increase in GLP-1 secretion from murine ileal cultures and were fully inhibited by the TRPA1 inhibitor HC-030031 (HC, 50 μmol/L). *C*: Incubation of carvacrol (Car, 50 μmol/L) in the presence of a complete voltage-gated ion channel block had no effect on GLP-1 secretion from murine ileal cultures; however, a significant increase in GLP-1 secretion was observed following a similar incubation with bombesin (Bom, 100 nmol/L) (n = 5–6, unpaired Student t test). *D–F*: The PUFAs AA, EPA, and DHA (all at 200 μmol/L) all caused robust and significant increases in GLP-1 secretion and were not affected by coincubation with HC (50 μmol/L). *G* and *H*: The effect of AITC and carvacrol to increase GLP-1 secretion from murine ileal cultures was abolished in *trpa1*$^{-/-}$ mice (black bars) compared with wild type (white bars). Experiments were $n \geq 6$ wells from three or more mice, unless otherwise indicated. */#$P < 0.05$, **/##$P < 0.01$, and ***/###$P < 0.001$, one-way ANOVA with Bonferroni post hoc test; *significance level from baseline, #significance level between groups. The dotted line on each graph represents the respective baseline value. n.s., not significant.

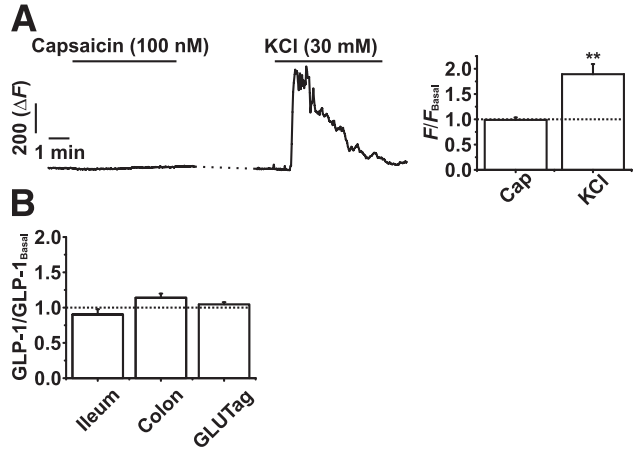

Figure 7—Analysis of functional TRPV1 in primary enteroendocrine cells and GLUTag cells. *A*: Addition of capsaicin (Cap, 100 nmol/L) failed to elicit any significant change in intracellular Ca^{2+} levels as measured by GCaMP3 fluorescence in colonic L cells from GLU-Cre/ROSA26-GCaMP3 mice. KCl (30 mmol/L) was used to confirm the responsiveness of each L cell analyzed. *B*: Incubation of murine ileal or colonic intestinal cultures or GLUTag cells with capsaicin (100 nmol/L) for 2 h did not significantly alter GLP-1 secretion compared with basal (10 mmol/L glucose). All experiments were $n \geq 5$. **$P < 0.01$, repeated-measures ANOVA or one-way ANOVA, both with Bonferroni post hoc test. The dotted line on each graph represents the respective baseline value.

as well as by PUFAs, and were largely abolished by TRPA1 antagonists or in mice lacking *trpa1*, clearly demonstrating a role for TRPA1 in GLP-1 secretion. Others have reported an elevation of murine plasma PYY after application of the TRPA1 agonists cinnamaldehyde or methyl syringate, which was blocked when ruthenium red or HC-030031 was coapplied (18). By contrast, although we observed an elevation of GLP-1 after AITC application in vivo, the effect was preserved in *trpa1*$^{-/-}$ mice. We believe that factors such as the relatively small effect size and the nonspecific targets of higher concentrations of AITC hindered the detection of significant TrpA1-mediated changes in plasma hormone concentrations. *Trpa1* was also detected in a recent RNASeq analysis of transcripts enriched in gastric D cells (A.E. Adriaenssens, F.M.G., F.R., unpublished data), suggesting that stimulation of D-cell somatostatin release might also be triggered by TRPA1 agonists in vivo, which would tend to counteract the secretion of GLP-1 (32).

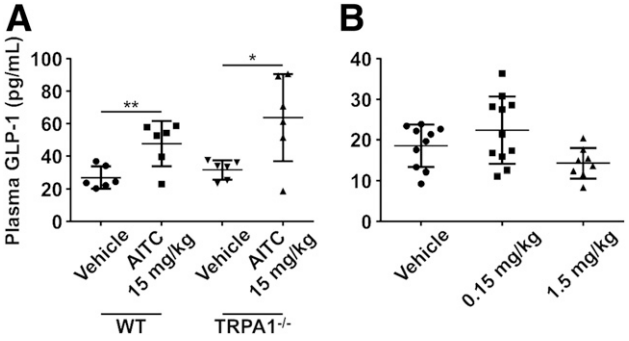

Figure 6—In vivo effects of AITC. *A*: Administration of AITC (15 mg/kg) or vehicle (PBS) by oral gavage caused a significant increase in plasma GLP-1 levels at 5 min in wild-type (WT) mice that was also present in the *trpa1*$^{-/-}$ (n = 6). *B*: The administration of AITC at 1.5 and 0.15 mg/kg failed to cause any significant increase in plasma GLP-1 levels (n = 8–11; two-way unpaired Student t test). *$P < 0.05$ and **$P < 0.01$.

TRPA1 channels are known to be activated by numerous dietary-related compounds such as those present in cinnamon, ginger, and oregano as well as the *Brassica* genus of plants. Besides stimulation by AITC and carvacrol, we found that TRPA1 channels in duodenal L cells were also activated by PUFAs, consistent with their putative role as a fatty acid sensor (19). Intracellular Ca^{2+} fluxes caused by AA, EPA, or DHA were fully or partially inhibited by the coapplication of a specific TRPA1 antagonist. By contrast, TRPA1 antagonism had either partial or no effect on PUFA-triggered GLP-1 secretion from GLUTag or primary ileal cultures, respectively. The reason for this discrepancy is unclear, but it could reflect differences in the duration of PUFA exposure between the experimental approaches. PUFAs, such as AA, have well-established roles in intracellular cell signaling and they are

an essential precursor of eicosanoid synthesis (33,34). These alternative pathways could contribute to an increase in GLP-1 secretion, independent of TRPA1 activation, potentially explaining the mismatch between PUFA-associated changes in cellular Ca^{2+} and GLP-1 release. The additional discrepancy between GLUTag and primary L cells, in terms of PUFA-induced GLP-1 secretion, could be due to the differences in the relative contributions of TRPA1-dependent and -independent mechanisms that are downstream of PUFA stimulation.

The finding of *trpa1* expression in upper small intestinal L cells is consistent with a recent report that *trpa1* was identified in cholecystokinin (CCK)-containing enteroendocrine cells of the mouse intestinal tract (35). Although the authors did not specifically examine whether *trpa1* was also coexpressed with GLP-1, we showed previously that approximately half of CCK-positive cells in the small intestine coexpress GLP-1 (27). In the present manuscript, we restricted our functional analysis to TRPA1, but further investigation is warranted into the roles of TRPC1, TRPC3, and TRPM7, which have putative functions in regulating intracellular Ca^{2+} levels by capacitative Ca^{2+} entry, or in Mg^{2+} homeostasis (36,37). Another TRP channel, TRPV1, was recently reported to play a role in enhancing GLP-1 and insulin secretion in mice (16), but whether this effect was via direct enteroendocrine cell activation was unclear. Our findings that capsaicin had no effect on intracellular Ca^{2+} levels in murine colonic L cells or on GLP-1 secretion and that the microarray signal for TRPV1 was very low in L cells suggest that TRPV1-associated GLP-1 secretion is not via direct activation of L cells. As TRPV1 activation has been shown to augment gastric emptying in both mice and humans (38,39), it is possible that the previously observed augmentation by capsaicin of glucose-triggered GLP-1 release was related to the rapid emptying of gastric glucose, delivering a larger glucose load to L cell–rich regions of the intestine.

Physiological Relevance

Based on the success of incretin-based strategies for the treatment for type 2 diabetes, new therapeutic approaches are under evaluation, aiming to stimulate the endogenous release of GLP-1 and other gut peptides. Evidence supporting this approach comes from the field of bariatric surgery, which is not only successful for the treatment of morbid obesity but additionally results in the remission of type 2 diabetes in many individuals. Rearrangement of the gastrointestinal tract during surgery limits or restricts food entering the stomach and/or the upper small intestine, exposing the unbypassed intestine to an enriched nutrient environment. Associated with this change in nutrient exposure are significantly elevated postprandial GLP-1 and PYY levels (40), which likely contribute to improved insulin release and reduced appetite. Developing strategies that medically mimic bariatric surgery is a high priority.

The role of TRPA1 in GLP-1 secretion in humans is yet to be studied, but there is emerging evidence that TRPA1 dietary agonists can participate in the restoration of glycemic control in patients with type 2 diabetes (41–44). A recent meta-analysis investigating the effects of dietary cinnamon, which contains the TRPA1 agonist cinnamaldehyde, showed that there was a significant improvement in levels of fasting plasma glucose, total cholesterol, and triglyceride levels after 4–18 weeks of increased cinnamon intake (45). Our findings offer support for the investigation of whether small intestinal delivery of TRPA1 dietary agonists can regulate glycemic control and present TRPA1 as a potential therapeutic target for the treatment of type 2 diabetes.

Acknowledgments. GLP-1 immunoassays were performed by Keith Burling at the Medical Research Council Metabolic Diseases Unit, Cambridge, U.K.

Funding. This work was supported by Wellcome Trust grants (WT088357/Z/09/Z and WT084210/Z/07/Z) and an MRC grant (MC_UU_12012/3) to F.R. and F.M.G.

Duality of Interest. F.R. has received speaker's fees from Merck Sharp & Dohme and Novo Nordisk and ad hoc consulting fees from AstraZeneca. F.M.G. has received speaker's fees from Novo Nordisk, Merck Sharp & Dohme, and Eli Lily and Company and ad hoc consulting fees from Roche and Pfizer. No other potential conflicts of interest relevant to this article were reported.

Author Contributions. E.C.E. initiated the project; designed the experiments; performed electrophysiology, calcium imaging, and GLP-1 secretion experiments; performed quantitative mRNA analyses; performed in vivo experiments; and wrote and edited the manuscript. E.D. performed quantitative mRNA analyses and in vivo experiments. C.G. provided the *trpa1*$^{-/-}$ mice and performed preliminary and in vivo experiments. A.P. performed in vivo experiments. A.M.H. performed FACS and microarray analysis. S.B. provided the *trpa1*$^{-/-}$ mice, performed preliminary experiments, and edited the manuscript. M.J.M.F. designed the experiments, performed in vivo experiments, and edited the manuscript. F.R. and F.M.G. designed the experiments and wrote and edited the manuscript. E.C.E. is the guarantor of this work and, as such, had full access to all the data in the study and takes responsibility for the integrity of the data and the accuracy of the data analysis.

References

1. Drucker DJ. Incretin action in the pancreas: potential promise, possible perils, and pathological pitfalls. Diabetes 2013;62:3316–3323

2. Drucker DJ, Nauck MA. The incretin system: glucagon-like peptide-1 receptor agonists and dipeptidyl peptidase-4 inhibitors in type 2 diabetes. Lancet 2006;368:1696–1705

3. DeFronzo RA, Ratner RE, Han J, Kim DD, Fineman MS, Baron AD. Effects of exenatide (exendin-4) on glycemic control and weight over 30 weeks in metformin-treated patients with type 2 diabetes. Diabetes Care 2005;28:1092–1100

4. Robinson LE, Holt TA, Rees K, Randeva HS, O'Hare JP. Effects of exenatide and liraglutide on heart rate, blood pressure and body weight: systematic review and meta-analysis. BMJ Open 2013;3:3

5. Ahrén B, Gomis R, Standl E, Mills D, Schweizer A. Twelve- and 52-week efficacy of the dipeptidyl peptidase IV inhibitor LAF237 in metformin-treated patients with type 2 diabetes. Diabetes Care 2004;27:2874–2880

6. Rhee NA, Vilsbøll T, Knop FK. Current evidence for a role of GLP-1 in Roux-en-Y gastric bypass-induced remission of type 2 diabetes. Diabetes Obes Metab 2012;14:291–298

7. Jørgensen NB, Dirksen C, Bojsen-Møller KN, et al. Exaggerated glucagon-like peptide 1 response is important for improved β-cell function and glucose tolerance after Roux-en-Y gastric bypass in patients with type 2 diabetes. Diabetes 2013;62:3044–3052

8. Ezcurra M, Reimann F, Gribble FM, Emery E. Molecular mechanisms of incretin hormone secretion. Curr Opin Pharmacol 2013;13:922–927

9. Rogers GJ, Tolhurst G, Ramzan A, et al. Electrical activity-triggered glucagon-like peptide-1 secretion from primary murine L-cells. J Physiol 2011;589:1081–1093

10. Tolhurst G, Zheng Y, Parker HE, Habib AM, Reimann F, Gribble FM. Glutamine triggers and potentiates glucagon-like peptide-1 secretion by raising cytosolic Ca2+ and cAMP. Endocrinology 2011;152:405–413
11. Diakogiannaki E, Pais R, Tolhurst G, et al. Oligopeptides stimulate glucagon-like peptide-1 secretion in mice through proton-coupled uptake and the calcium-sensing receptor. Diabetologia 2013;56:2688–2696
12. Tolhurst G, Heffron H, Lam YS, et al. Short-chain fatty acids stimulate glucagon-like peptide-1 secretion via the G-protein-coupled receptor FFAR2. Diabetes 2012;61:364–371
13. Venkatachalam K, Montell C. TRP channels. Annu Rev Biochem 2007;76:387–417
14. Zhang Y, Hoon MA, Chandrashekar J, et al. Coding of sweet, bitter, and umami tastes: different receptor cells sharing similar signaling pathways. Cell 2003;112:293–301
15. Boesmans W, Owsianik G, Tack J, Voets T, Vanden Berghe P. TRP channels in neurogastroenterology: opportunities for therapeutic intervention. Br J Pharmacol 2011;162:18–37
16. Wang P, Yan Z, Zhong J, et al. Transient receptor potential vanilloid 1 activation enhances gut glucagon-like peptide-1 secretion and improves glucose homeostasis. Diabetes 2012;61:2155–2165
17. Cao DS, Zhong L, Hsieh TH, et al. Expression of transient receptor potential ankyrin 1 (TRPA1) and its role in insulin release from rat pancreatic beta cells. PLoS ONE 2012;7:e38005
18. Kim MJ, Son HJ, Song SH, Jung M, Kim Y, Rhyu MR. The TRPA1 agonist, methyl syringate suppresses food intake and gastric emptying. PLoS ONE 2013;8:e71603
19. Motter AL, Ahern GP. TRPA1 is a polyunsaturated fatty acid sensor in mammals. PLoS ONE 2012;7:e38439
20. Xu H, Delling M, Jun JC, Clapham DE. Oregano, thyme and clove-derived flavors and skin sensitizers activate specific TRP channels. Nat Neurosci 2006;9:628–635
21. Hlebowicz J, Hlebowicz A, Lindstedt S, et al. Effects of 1 and 3 g cinnamon on gastric emptying, satiety, and postprandial blood glucose, insulin, glucose-dependent insulinotropic polypeptide, glucagon-like peptide 1, and ghrelin concentrations in healthy subjects. Am J Clin Nutr 2009;89:815–821
22. Kwan KY, Allchorne AJ, Vollrath MA, et al. TRPA1 contributes to cold, mechanical, and chemical nociception but is not essential for hair-cell transduction. Neuron 2006;50:277–289
23. Parker HE, Adriaenssens A, Rogers G, et al. Predominant role of active versus facilitative glucose transport for glucagon-like peptide-1 secretion. Diabetologia 2012;55:2445–2455
24. Zariwala HA, Borghuis BG, Hoogland TM, et al. A Cre-dependent GCaMP3 reporter mouse for neuronal imaging in vivo. J Neurosci 2012;32:3131–3141
25. Luche H, Weber O, Nageswara Rao T, Blum C, Fehling HJ. Faithful activation of an extra-bright red fluorescent protein in "knock-in" Cre-reporter mice ideally suited for lineage tracing studies. Eur J Immunol 2007;37:43–53
26. Reimann F, Habib AM, Tolhurst G, Parker HE, Rogers GJ, Gribble FM. Glucose sensing in L cells: a primary cell study. Cell Metab 2008;8:532–539
27. Habib AM, Richards P, Cairns LS, et al. Overlap of endocrine hormone expression in the mouse intestine revealed by transcriptional profiling and flow cytometry. Endocrinology 2012;153:3054–3065
28. Psichas A, Sleeth ML, Murphy KG, et al. The short chain fatty acid propionate stimulates GLP-1 and PYY secretion via free fatty acid receptor 2 in rodents. Int J Obes (Lond). 11 August 2014 [Epub ahead of print]
29. Story GM, Peier AM, Reeve AJ, et al. ANKTM1, a TRP-like channel expressed in nociceptive neurons, is activated by cold temperatures. Cell 2003;112:819–829
30. Reimann F, Gribble FM. Glucose-sensing in glucagon-like peptide-1-secreting cells. Diabetes 2002;51:2757–2763
31. Everaerts W, Gees M, Alpizar YA, et al. The capsaicin receptor TRPV1 is a crucial mediator of the noxious effects of mustard oil. Curr Biol 2011;21:316–321
32. Moss CE, Marsh WJ, Parker HE, et al. Somatostatin receptor 5 and cannabinoid receptor 1 activation inhibit secretion of glucose-dependent insulinotropic polypeptide from intestinal K cells in rodents. Diabetologia 2012;55:3094–3103
33. Khan WA, Blobe GC, Hannun YA. Arachidonic acid and free fatty acids as second messengers and the role of protein kinase C. Cell Signal 1995;7:171–184
34. Hwang SC, Jhon DY, Bae YS, Kim JH, Rhee SG. Activation of phospholipase C-gamma by the concerted action of tau proteins and arachidonic acid. J Biol Chem 1996;271:18342–18349
35. Cho HJ, Callaghan B, Bron R, Bravo DM, Furness JB. Identification of enteroendocrine cells that express TRPA1 channels in the mouse intestine. Cell Tissue Res 2014;356:77–82
36. Cheng KT, Ong HL, Liu X, Ambudkar IS. Contribution and regulation of TRPC channels in store-operated Ca2+ entry. Curr Top Membr 2013;71:149–179
37. Ryazanova LV, Rondon LJ, Zierler S, et al. TRPM7 is essential for Mg(2+) homeostasis in mammals. Nat Commun 2010;1:109
38. Debreceni A, Abdel-Salam OM, Figler M, Juricskay I, Szolcsányi J, Mózsik G. Capsaicin increases gastric emptying rate in healthy human subjects measured by ^{13}C-labeled octanoic acid breath test. J Physiol Paris 1999;93:455–460
39. Medeiros JV, Bezerra VH, Lucetti LT, et al. Role of KATP channels and TRPV1 receptors in hydrogen sulfide-enhanced gastric emptying of liquid in awake mice. Eur J Pharmacol 2012;693:57–63
40. Peterli R, Wölnerhanssen B, Peters T, et al. Improvement in glucose metabolism after bariatric surgery: comparison of laparoscopic Roux-en-Y gastric bypass and laparoscopic sleeve gastrectomy: a prospective randomized trial. Ann Surg 2009;250:234–241
41. Lu T, Sheng H, Wu J, Cheng Y, Zhu J, Chen Y. Cinnamon extract improves fasting blood glucose and glycosylated hemoglobin level in Chinese patients with type 2 diabetes. Nutr Res 2012;32:408–412
42. Akilen R, Tsiami A, Devendra D, Robinson N. Glycated haemoglobin and blood pressure-lowering effect of cinnamon in multi-ethnic Type 2 diabetic patients in the UK: a randomized, placebo-controlled, double-blind clinical trial. Diabet Med 2010;27:1159–1167
43. Solomon TP, Blannin AK. Effects of short-term cinnamon ingestion on in vivo glucose tolerance. Diabetes Obes Metab 2007;9:895–901
44. Solomon TP, Blannin AK. Changes in glucose tolerance and insulin sensitivity following 2 weeks of daily cinnamon ingestion in healthy humans. Eur J Appl Physiol 2009;105:969–976
45. Allen RW, Schwartzman E, Baker WL, Coleman CI, Phung OJ. Cinnamon use in type 2 diabetes: an updated systematic review and meta-analysis. Ann Fam Med 2013;11:452–459